Analysis of new experimental data on the ^{160}Dy spectrum with the symplectic interacting vector boson model

A. A. Solnyshkin,[1] V. P. Garistov,[1,2] A. Georgieva,[2] H. Ganev,[2] and V. V. Burov[1]
[1]*Joint Institute for Nuclear Research, Dubna, Russia*
[2]*Institute for Nuclear Research and Nuclear Energy, BAS, Sofia, Bulgaria*
(Received 12 August 2005; published 22 December 2005)

Analysis of the recently obtained experimental data for a lot of collective states of ^{160}Dy is presented. Classification of the low-lying states with positive parity $0^+, 2^+, 4^+, 6^+$ is performed. The energies of rotational high-spin states of the ground, S, γ and two negative-parity bands are described in the framework of the interacting vector boson model. The energies of the bands are reproduced with high accuracy using only one set of model parameters for all bands. A more detailed investigation of the results is performed by calculation and comparison with experiment of the high-order odd-even staggering effects between states from different pairs of bands.

DOI: 10.1103/PhysRevC.72.064321 PACS number(s): 27.70.+q, 21.10.Re, 23.20.Lv

I. INTRODUCTION

The even-even nucleus ^{160}Dy has a very complicated spectrum of excited states and by now it has been widely investigated experimentally. During the past decades, a great number of experiments have been performed using different types of nuclear reactions, including Coulomb excitation and β decay (^{160}Tb $\rightarrow$ ^{160}Dy, $^{160\mathrm{m,g}}$Ho $\rightarrow$ ^{160}Dy, ^{160}Er $\rightarrow$ $^{160\mathrm{m,g}}$Ho $\rightarrow$ ^{160}Dy). The results of all the investigations performed up to 1996 were analyzed in detail and presented in Nuclear Data Sheets [1] and *Table of Isotopes* [2]. Nevertheless, recently, using modern experimental techniques, a new comprehensive study of the low-spin states in the β decay ^{160}Er $\rightarrow$ $^{160\mathrm{m,g}}$Ho $\rightarrow$ ^{160}Dy had been performed, measuring γ rays, conversional electrons, and $\gamma\gamma t$ coincidence spectra [3]. These investigations had supplemented the spectrum of the excited states of ^{160}Dy with more than 100 states and more than 500 γ transitions. The agreement with the data obtained from previous experiments with nuclear reactions and β decay also was checked. At the same time a new experiment using a ^{7}Li ion beam on a ^{158}Gd target has been done [4] to obtain more high-spin states in the spectrum of ^{160}Dy. For example, the ground-state bands with $K^\pi = 0^+$ were identified up to excitation energy of 7231 keV and $I^\pi = 28^+$, a γ band with $K^\pi = 2^+$ was measured up to energy 6642 keV and $I^\pi = 25^+$, an S band was measured up to 4875 keV with $I^\pi = 20^+$, and two negative-parity bands with $K^\pi = 2^-$ were measured up to energy 6967 keV with $I^\pi = 26^-$ and with $K^\pi = 1^-$ up to energy 4937 keV with $I^\pi = 19^-$. In these new experiments, 16 other, different in nature rotational bands were identified in the ^{160}Dy nucleus. All this made the spectrum of this nucleus a very good target for testing theoretical nuclear structure models. An attempt to analyze it was recently made [5], by applying the Bohr-Mottelson model [6], Q-phonon model [7], variable moment of inertia model with dynamical asymmetry [8], and the Bohr-Mottelson model with Coriolis interaction [9]. Also, the positive-parity states were analyzed within the framework of the algebraic IBM-1 [10]. Within those model approaches a relatively good description for the energies and transition probabilities of states with low values of their assigned spins was obtained, but the disagreement with experiment increased noticeably in the region of higher spin values. As a continuation of our theoretical analysis of the very rich experimental data on ^{160}Dy, we apply in the present paper two of the recently developed dynamical symmetries in the symplectic extension of the interacting vector boson model (IVBM) [11,12]. Our aim is twofold:

(i) to describe the energy distribution of the low-lying states with $J^\pi = 0^+, 2^+, 4^+$, and 6^+ most of which are band heads and play a very important role in the development of the collective bands on them, and
(ii) to extend the energy description to the higher spin states in the collective bands and at the same time to check their assignment to the respective collective bands.

The phenomenological IVBM [11] was proven appropriate for a rather accurate description of the low-lying spectra of even-even well-deformed nuclei. The most general spectrum-generating algebra of the model is the algebra of the Sp(12, R) group [12]. It has a rather rich subalgebraic structure. In the rotational limit of the model the reduction of sp(12, R) to the angular momentum algebra so(3) was carried out through the compact u(6) subalgebra, which defines the number of boson preserving version of the model. Another new reduction of the dynamical sp(12, R) symmetry algebra to the direct product sp(4, R) $\otimes$ so(3) isolates states with fixed angular momentum L [13]. This permits an investigation of the behavior of low-lying collective states with the same angular momentum L with respect to the number of excitations N building these states. These two new dynamical symmetries of the symplectic IVBM,

$$\begin{array}{ccccc} \mathrm{sp}(12,R) & \supset & \mathrm{sp}(4,R) & \otimes & \mathrm{so}(3) \\ \cup & & \cup & & \cap \\ \mathrm{u}(6) & \supset & \mathrm{u}(2) & \otimes & \mathrm{su}(3), \end{array} \tag{1}$$

afford a natural way to change the number of "phonons," and relation (1) can be used to link different sets of states. This is the main feature of the model and one that underpins its application, which will be used here to interpret the new experimental results in the ^{160}Dy spectrum. In this paper we take a more empirical approach in reaching our goals,

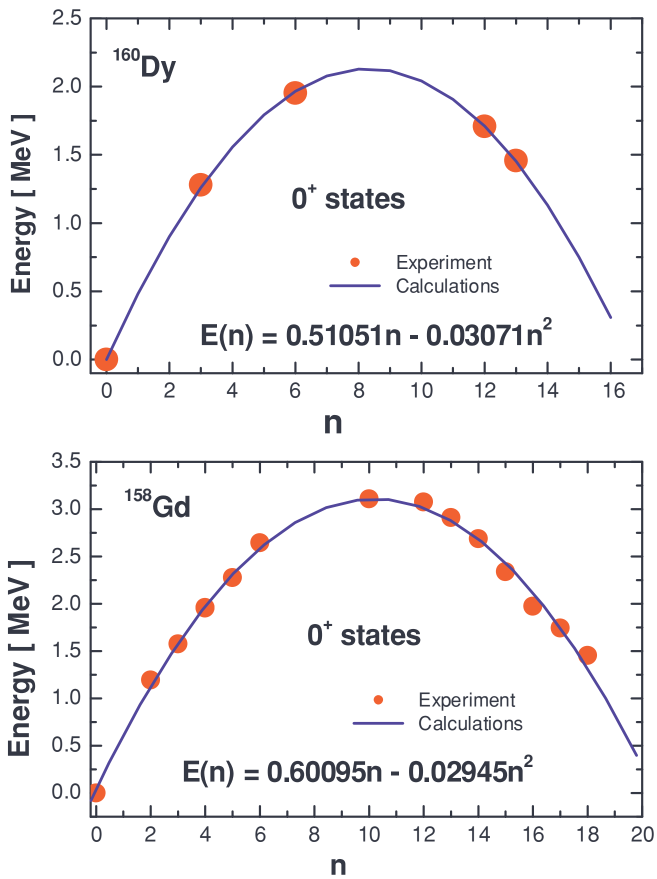

FIG. 1. (Color online) Distribution of 0^+ states energies by number of monopole bosons in ^{160}Dy and ^{158}Gd.

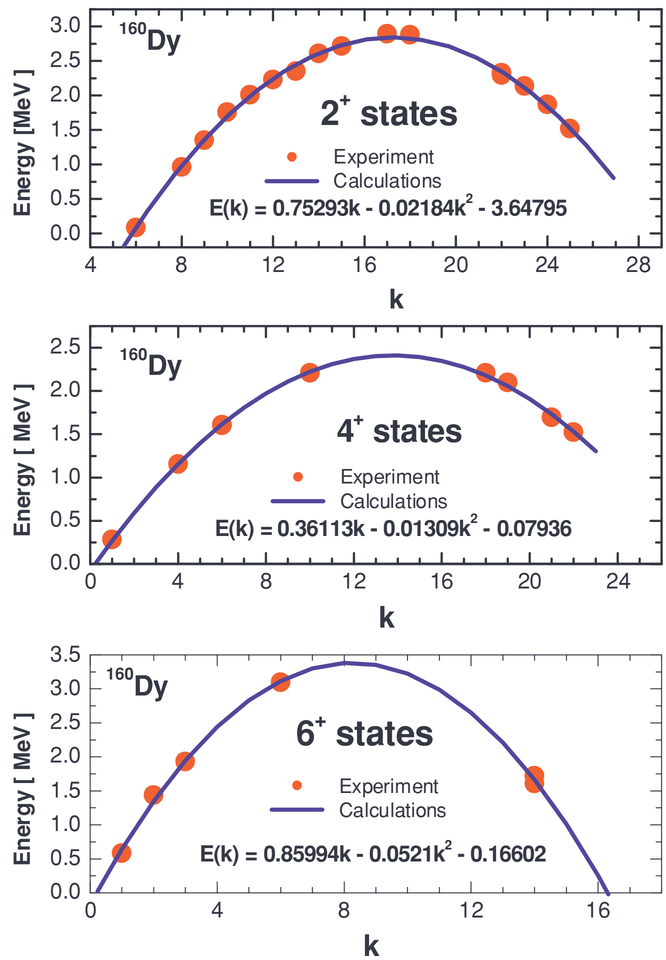

FIG. 2. (Color online) Distribution of $2^+, 4^+$, and 6^+ states energies by number of bosons within IVBM ($k = N/4$).

introducing in this way more of the physical interpretation of the experimental data. This approach is theoretically backed up by the IVBM and the group-theoretical techniques is used mainly to classify the observed collective states with respect to the quantum numbers that label the representations of the subgroups of the considered dynamical symmetries (1).

II. ENERGY DISTRIBUTION OF THE EXCITED 0^+ STATES

We start our investigations of the experimental spectrum of ^{160}Dy with the study of the low-lying 0^+ states. This is very important as all these states are band heads of collective bands and to a great extent influence their development. First we make a classification of the observed 0^+ states within the framework of the simplified pairing vibrational model by making use of a phenomenological collective Hamiltonian written in terms of the operators R_+, R_-, and R_0:

$$H = \alpha R_+ R_- + \beta R_0 \left(R_0 + \frac{\Omega}{2} \right), \tag{2}$$

where α and β are model parameters. The monopole bosons R_+, R_-, and R_0 are constructed from pairs of fermion creation and annihilation operators $a^\dagger_{jm}$ and a_{jm}, where $(a^\dagger_{jm})^\dagger = (-1)^m a_{j-m}$ for particles placed on a single j-level (where j = half integer) with projection m and $\Omega = (2j + 1/2)$:

$$\begin{aligned} R_+ &= \frac{1}{2}\sum_m (-1)^{j-m} \alpha^\dagger_{jm} \alpha^\dagger_{j-m}, \\ R_- &= \frac{1}{2}\sum_m (-1)^{j-m} \alpha_{j-m} \alpha_{jm}, \\ R_0 &= \frac{1}{4}\sum_m (\alpha^\dagger_{jm}\alpha_{jm} - \alpha_{j-m}\alpha^\dagger_{j-m}), \\ [R_0, R_\pm] &= \pm R_\pm, \quad [R_+, R_-] = 2R_0. \end{aligned} \tag{3}$$

By applying the Holstein-Primakoff [14] transformation to the operators R_+, R_-, and R_0 they are expressed in terms of new (ideal) boson creation and annihilation operators $b^\dagger, b$ as

$$\begin{aligned} R_- &= (\sqrt{2\Omega - b^\dagger b})b, \quad R_+ = b^\dagger(\sqrt{2\Omega - b^\dagger b}), \\ R_0 &= b^+ b - \Omega. \end{aligned} \tag{4}$$

These new operators $b^\dagger, b$ commute as

$$[b, b^\dagger] = 1, \quad [b, b] = [b^\dagger, b^\dagger] = 0. \tag{5}$$

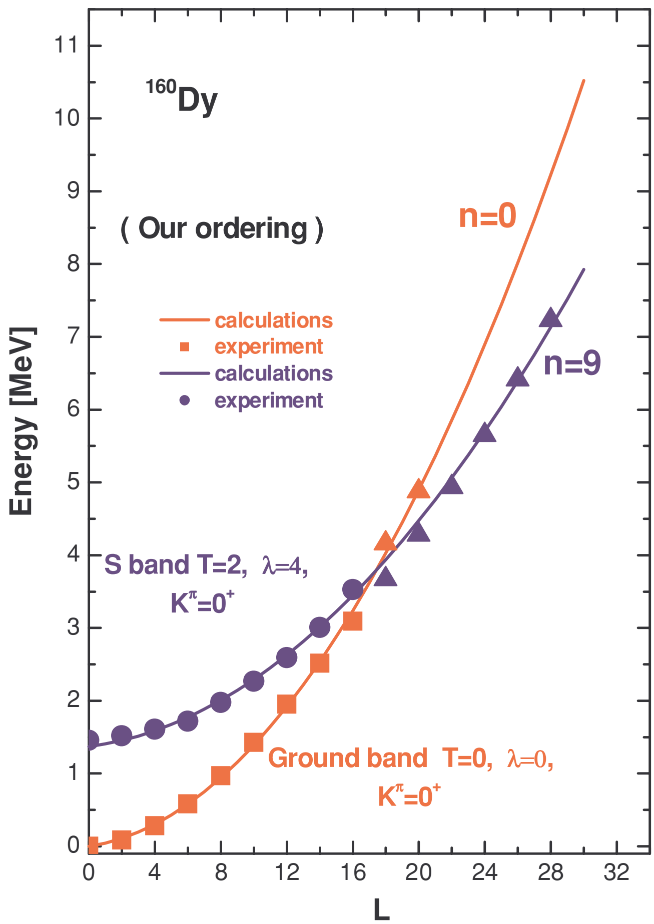

FIG. 3. (Color online) Comparison of IVBM energies with experiment for the ground and S bands in ^{160}Dy.

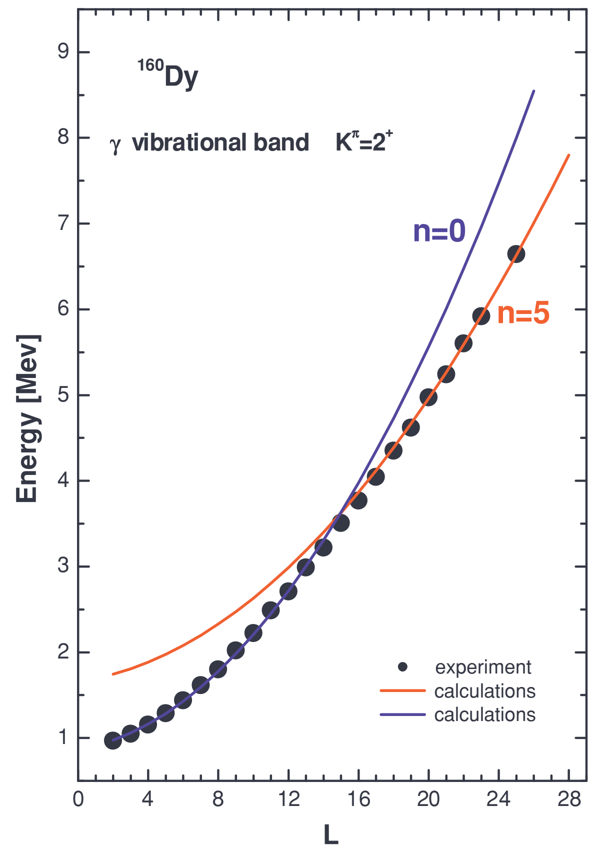

FIG. 4. (Color online) Comparison of IVBM energies with experiment for γ band in ^{160}Dy.

The initial Hamiltonian (2) written in terms of the ideal bosons $b^{\dagger}$, b has the form

$$H = Ab^{\dagger}b - Bb^{\dagger}bb^{\dagger}b, \tag{6}$$

and the new constants of the one- and two-body interactions are

$$A = \alpha(2\Omega + 1) - \beta\Omega, \quad B = \alpha - \beta.$$

The boson state $|n\rangle$ is built by the scalar bosons in a standard way as

$$|n\rangle = \frac{1}{\sqrt{n!}}(b^{+})^{n}\,|0\rangle\,, \tag{7}$$

with the vacuum state defined by $b\,|0\rangle = 0$. Thus the energy spectrum of the 0^{+} states produced by the Hamiltonian (6) is a parabolic function of the number of ideal monopole bosons $n = b^{\dagger}b$ that build them:

$$E_n = An - Bn^2. \tag{8}$$

In Fig. 1 we show the energy distribution of available experimental data for 0^{+} states in the spectrum of ^{160}Dy with respect to the number of ideal monopole bosons (5). In the same figure as an additional example we present our results for the description of 0^{+} excited states in the new experimental data for the ^{158}Gd nucleus [15]. The parameters A and B of (8) are evaluated by fitting the experimental energies of the different 0^{+} states to the theoretical ones for all possible permutations of the classification numbers n attributed to each 0^{+} state. The distribution corresponding to the minimal value of χ^2 is presented in Fig. 1. The mean square energy deviation Δ is 4.8 keV for ^{160}Dy and 16.7 keV for ^{158}Gd. Hence with rather high accuracy the experimental energies for low-lying 0^{+} collective states follow a parabolic distribution as functions of the number of collective excitations that build them. Now we can label each of the $K^{\pi} = 0^{+}$ states with an additional characteristic n—the number of monopole bosons determining their collective structure. An important point of this investigation is that the ordering of the states with respect to the number of phonons does not necessarily correspond to an increase of their excitation energy. For example, in the ^{160}Dy spectrum the third and fourth excited $K^{\pi} = 0^{+}$ states have more collective structure (lager $n = 12, 13$, respectively) than the 0^{+} state with highest excitation energy with corresponding $n = 6$. There are more demonstrative cases in the ^{158}Gd nucleus. A similar analysis can be performed for the other low-lying excited states with angular momenta different from zero. It shows that they can also be distributed on parabolic functions $E_k = Ak - Bk^2 + C$, with an additional free parameter C. Hence the new classification parameter k can also be considered as a measure of collectivity determining each low-lying collective state.

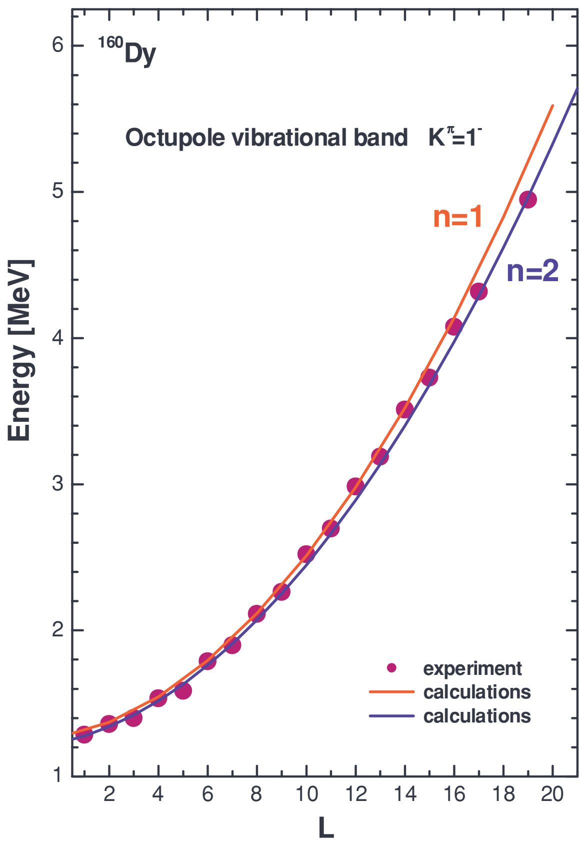

FIG. 5. (Color online) Comparison of IVBM energies with experiment for the octupole $K^{\pi} = 1^-$ band in ^{160}Dy.

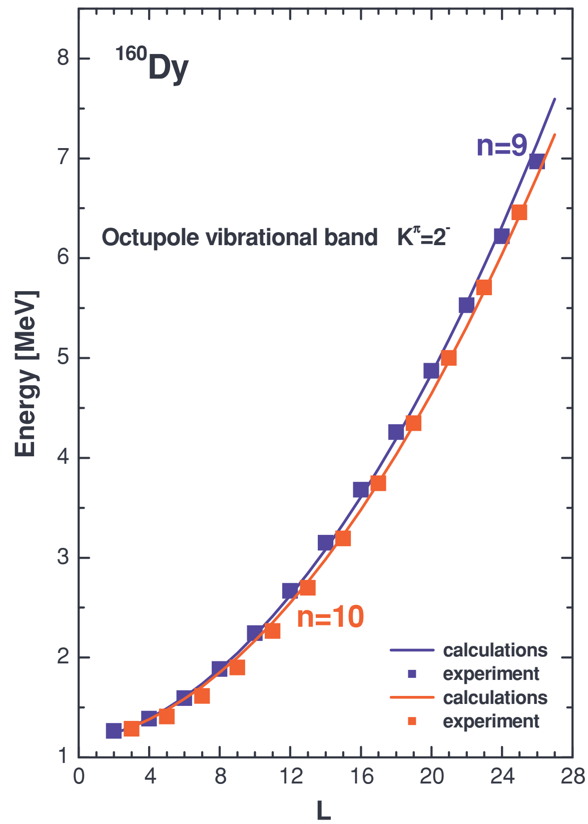

FIG. 6. (Color online) Comparison of IVBM energies with experiment for the octupole $K^{\pi} = 2^-$ band in ^{160}Dy.

In Fig. 2 we show the distributions of the $2^+, 4^+$, and 6^+ excited states in ^{160}Dy with respect to k. In all these cases we obtain good descriptions of the energy distributions of the respective states with mean square energy deviation $\Delta = 9.5$, 7.5, and 23.0 keV for the levels with $J^{\pi} = 2^+, 4^+$, and 6^+, respectively. The results introduced here illustrate that the theory reproduces reliably empirical observations of the energy distribution of collective states. Such a demonstration can be provided for any collective model that includes one- and two-body interactions in the Hamiltonian. The same feature that leads to this type of parametrization is provided by the symplectic dynamical symmetry of the IVBM [13], which allows for a change in the number of "phonons" that are required to build the states with any value of the angular momentum $L = 0, 1, 2, 3, 4, \ldots$, but from the building blocks of the model. In the reduction of sp(12, R) to the direct product Sp(4, R) ⊗ SO(3), the so(3) angular momentum algebra, through its complementary role, to sp(4, R), labels states with a fixed angular momentum L [13]. The Sp(4, R) basis is obtained via a reduction of its boson representations into the irreducible ones of SU(2), which are labeled by the quantum numbers T, T_0 of the pseudospin and its third projection. The first-order invariant of the U(2) ⊂ Sp(4, R) is the total number of vector bosons N of the IVBM. Further one exploits the relation (1) of this reduction to the reduction of sp(12, R) to its maximal compact subgroup U(6) ⊃ U(2) ⊗ SU(3), which gives the rotational limit of the IVBM. In further considerations we have established a relation between the IVBM quantum number N and the new positive-integer classification parameter k as $N = 4k$ [11]. This relates the sp(12, R) phenomenological collective model to a simple microscopic description of the collective states given in the foregoing discussion. We use the former here, as our main interest is in the influence of the 0^+ band heads' configurations on the development of the collective bands.

III. THE IVBM

We start with a brief introduction of the rotational limit of the model, where within the framework of the boson representation of the sp(12, R) algebra all possible irreducible representations $[N]_6$ of its maximal compact subgroup U(6) are realized. Further, their reduction to the irreps (λ, μ) of the group SU(3) are determined uniquely through all possible sets of the eigenvalues of the Hermitian operators N—the total number of bosons, T^2, and T_0—characterizing the "psuedospin," introduced to distinguish the two types of vector bosons, which are the building blocks of the algebraic structure of the model. In the final reduction of the (λ, μ) labels to the SO(3) representations,

$$\mathrm{sp}(12, R) \supset \underset{[N]_6}{\mathrm{u}(6)} \supset \underset{(\lambda, \mu)}{\mathrm{su}(3)} \otimes \underset{T, T_0}{\mathrm{SU}(2)} \supset \underset{L,}{\mathrm{so}(3)} \qquad (9)$$

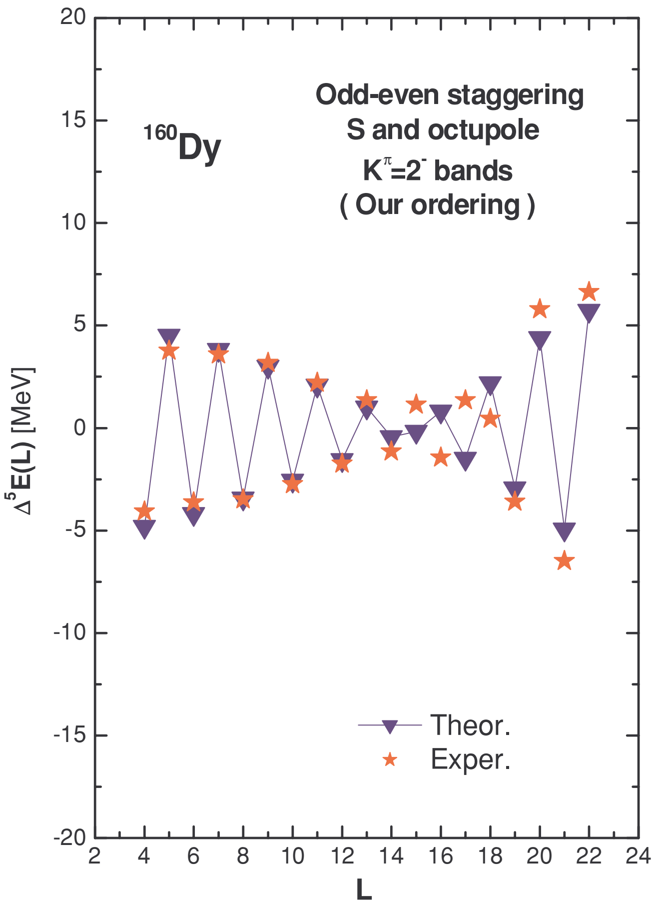

FIG. 7. (Color online) Comparison of theoretical and experimental staggering functions $\Delta^5 E\,(L)$ for S and octupole $K^\pi = 2^-$ bands of ^{160}Dy.

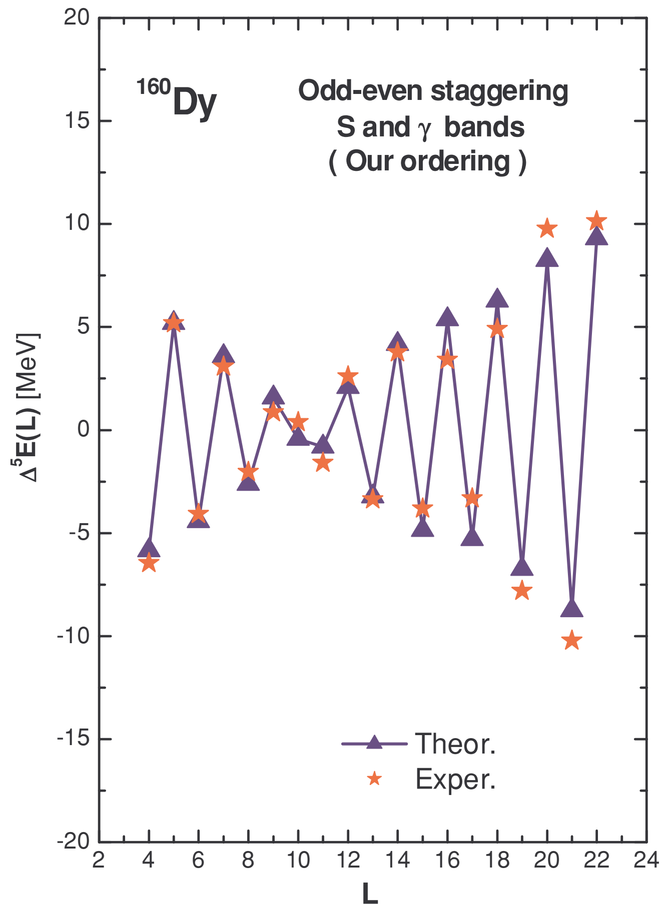

FIG. 8. (Color online) Comparison of theoretical and experimental staggering functions $\Delta^5 E\,(L)$ for S and $K^\pi = 2^+\gamma$ bands of ^{160}Dy.

the physical angular momentum L and its projection M are obtained. Hence the sp(12, R) plays the role of a group of dynamical symmetry. The detail description of this algebraic model may be found in [12]. Here we present only those expressions necessary for our purposes for the energy spectrum, given by the eigenvalues of the first- and second-order invariants of the subgroups of the chain,

$$\begin{aligned} &E([N]_6, (\lambda, \mu); L; T_0) \\ &\quad = \alpha N + \alpha_1 N(N+5) + \beta_3 L(L+1) \\ &\qquad + \alpha_3(\lambda^2 + \mu^2 + \lambda\mu + 3\lambda + 3\mu) + \alpha_1 T_0^2, \end{aligned} \tag{10}$$

and the decomposition rules for the states labels given by the irreducible representations of the subgroups in the model chain (9),

$$N - \text{even} \rightarrow 0, 2, 4, 6, \ldots \tag{11}$$

$$T = \frac{N}{2}, \frac{N}{2} - 1, \frac{N}{2} - 2, \ldots, 0, \text{or} 1, \tag{12}$$

$$T_0 = -T, -T+1, \ldots, T. \tag{13}$$

Because of the mutual complementarity of the su(3) and SU(2) the (λ, μ) labels are related:

$$\begin{aligned} \lambda &= 2T, \\ \mu &= \frac{N}{2} - T. \end{aligned} \tag{14}$$

Finally, the angular momentum labels are given in a standard way:

$$\begin{aligned} K &= \min(\lambda, \mu), \min(\lambda, \mu) - 2, \ldots, 0 \text{ or } 1, \\ K &= 0 \rightarrow L = 0, 2, \ldots, \max(\lambda, \mu), \\ K &\neq 0 \rightarrow L = \max(\lambda, \mu), \max(\lambda, \mu) - 1, \ldots, 0 \text{ or } 1. \end{aligned}$$

The parity of the states is defined as $\pi = (-1)^T$. The index K appearing in this reduction is related to the projection of L in the body-fixed frame and is used with the parity to label the different bands in the energy spectra of the nuclei. Now we have to obtain the correspondence between the observed collective bands and the eigenstates of the Hamiltonian that give the spectrum of the nucleus.

For this purpose we must choose the su(3) multiplets (λ, μ) determining the energies of the bands under consideration. Further imposing the connection $N = 4L$ we have the corresponding multiplets (λ, μ) and the expressions for energies of some rotational bands as follows:

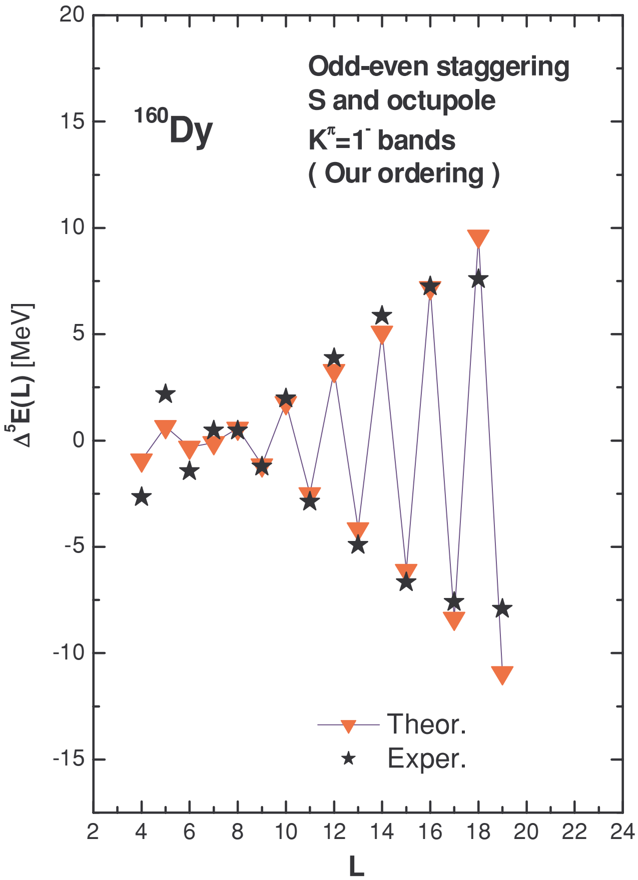

FIG. 9. (Color online) Comparison of theoretical and experimental staggering functions $\Delta^5 E(L)$ for S and octupole $K^\pi = 1^-$ bands of ^{160}Dy.

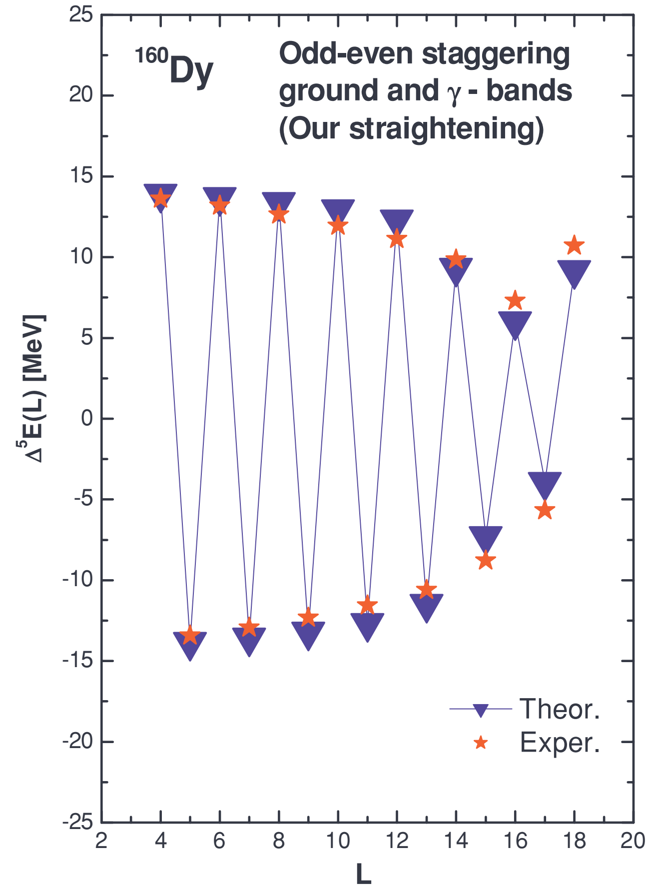

FIG. 10. (Color online) Comparison of theoretical and experimental staggering functions $\Delta^5 E(L)$ for ground $K^\pi = 0^+$ and $K^\pi = 2^+\gamma$ bands of ^{160}Dy.

(i) $K^\pi = 0^+$ ground-state band $\rightarrow (\lambda = 0, \mu = 2L)$ and $T = 0$:

$$E_{\rm gr} = 4\alpha L + \beta_3 L(L+1) + 4\alpha_1 L(5+4L) + \alpha_3(6L+4L^2);$$

(ii) $K^\pi = 0^+$ S band $\rightarrow (\lambda = 4, \mu = 2L-2)$ and $T = 2$:

$$E_s = c_s + 4\alpha L + \beta_3 L(L+1) + 4\alpha_1 L(5+4L) + \alpha_3(6L+4L^2);$$

(iii) $K^\pi = 1^-$ band $\rightarrow (\lambda = 4L-2, \mu = 1)$ and $T = 2L-1$:

$$E_{1^-} = c_{1^-} + 4\alpha L + \beta_3 L(L+1) + 4\alpha_1 L(5+4L) + \alpha_3[16L - 4 + (4L-2)^2]; \quad (15)$$

(iv) $K^\pi = 2^-$ band $\rightarrow (\lambda = 2, \mu = 2L-1)$ and $T = 1$:

$$E_{2^-} = c_{2^-} + 4\alpha L + \beta_3 L(L+1) + 4\alpha_1 L(5+4L) + \alpha_3[16L - 4 + (4L-2)^2].$$

(v) $K^\pi = 2^+ - \gamma$-band $\rightarrow (\lambda = 4L-4, \mu = 2)$ and $T = 2L-2$:

$$E_\gamma = c_\gamma + 4\alpha L + \beta_3 L(L+1) + 4\alpha_1 L(5+4L) + \alpha_3[20L - 10 + 16(L-1)^2].$$

Our previous calculations of rotational band energies with different forms of nuclear density shapes [11] had shown that the moment of inertia depends on the number of monopole bosons n approximately as

$$I(n) \approx I(0)(1 + xn), \quad (16)$$

where x is connected with the diffuseness parameter s, compressibility coefficient C_0, one-phonon energy E_0, and nuclear half-radius R as

$$x = \frac{E_0 R^2 [(-3+20\pi)R^4 + 30(-1+4\pi)R^2 s^2 + 45(-1+4\pi)s^4]}{8C_0\pi^2(R^6 + 13R^4 s^2 + 45R^2 s^4 + 45 s^6)}. \quad (17)$$

In our further calculations we suppose that the monopole excitations mainly determine the value of the moment of inertia and choose the parameter β_3 to be

$$\beta_3 = \frac{1}{2I(n)} = \frac{\beta_0}{1+nx}. \quad (18)$$

We apply this approximation in our calculations of the energies of rotational bands determined here (15).

The comparison of our calculations with experiment is shown in Figs. 3–6. It is important to point out that all these

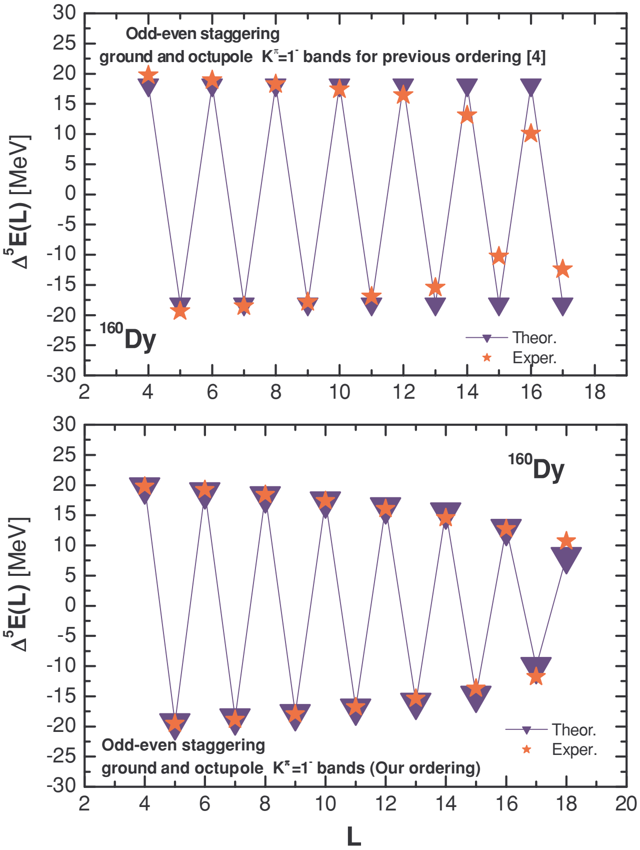

FIG. 11. (Color online) Comparison of the theoretical and experimental staggering functions $\Delta^5 E(L)$ for ground $K^\pi = 0^+$ (in the case of our states' ordering and the ordering in [4]) and octupole $K^\pi = 1^-$ bands of ^{160}Dy.

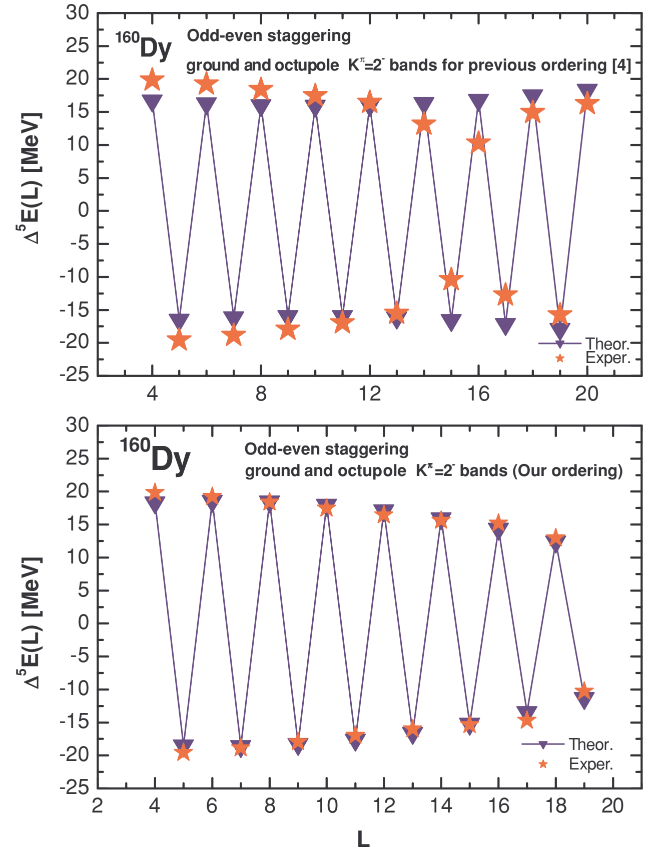

FIG. 12. (Color online) Comparison of theoretical and experimental staggering functions $\Delta^5 E(L)$ for ground $K^\pi = 0^+$ (in the case of our ordering and the ordering in [4]) and octupole $K^\pi = 2^-$ bands of ^{160}Dy.

bands are calculated with the same set of parameters:

$$\alpha = 0.00511953, \quad \alpha_1 = 0.000045, \quad \alpha_3 = -0.0001486, \tag{19}$$
$$x = 0.0605, \quad \beta_0 = 0.01117379.$$

The corresponding values of number of monopole bosons n building the collective excited 0^+ state are also presented in these figures. The values of n entering (18) according to our proposition mainly determine the moment of inertia of each band. The agreement between calculated and experimental energies is very good and the mean square energy deviation Δ for all bands under consideration is less than 9 keV per point. However, we consider the values c_s, c_{1^-}, c_{2^-}, and c_γ as free model parameters, but there are reasons to suppose that including the interactions among rotational bands will bring about one common constant for all bands.

For correct placement of the states in the bands with different parities and to check the parity splitting we have calculated the fifth-order staggering functions

$$\begin{aligned}\Delta^5 E(L) = {} & 6[E(L) - E(L-1)] - 4[E(L-1) - E(L-2)] \\ & - 4[E(L+1) - E(L)] + E(L+2) - E(L+1) \\ & + E(L-2) - E(L-3) \end{aligned} \tag{20}$$

for experimental points and calculated data.

According to our calculations for the energies of the bands (Figs. 3–6) we had calculated the staggering functions with replaced states $I^\pi = 18^+$, 4.181 MeV; $I^\pi = 20^+$, 4.875 MeV from the S band to the ground band (our ordering) whereas the states $I^\pi = 18^+$, 3.67 MeV; $I^\pi = 20^+$, 4.279 MeV; $I^\pi = 22^+$, 4.936 MeV; $I^\pi = 24^+$, 5.648 MeV; $I^\pi = 26^+$, 6.413 MeV; $I^\pi = 28^+$, 7.231 MeV from the ground-state to the S band. This produces much better agreement with experiment than the calculations with the previous ordering [4]. Hence we have proposed that the sequence of states $I^\pi = 18^+$, 4.181 MeV; $I^\pi = 20^+$, 4.875 MeV belongs to the ground-state band whereas the states $I^\pi = 18^+$, 3.67 MeV; $I^\pi = 20^+$, 4.279 MeV; $I^\pi = 22^+$, 4.936 MeV; $I^\pi = 24^+$, 5.648 MeV; $I^\pi = 26^+$, 6.413 MeV; $I^\pi = 28^+$, 7.231 MeV must be related to the S band; moreover, for simultaneous description of the bands with previous ordering [4] the additional parameter is required. The odd-even staggering functions (20) for S ($K^\pi = 0^+$) and octupole ($K^\pi = 2^-$) bands, S ($K^\pi = 0^+$) and $\gamma(K^\pi = 2^+)$ bands, S ($K^\pi = 0^+$) and octupole ($K^\pi = 1^-$) bands, and ground ($K^\pi = 0^+$) and γ ($K^\pi = 2^+$) bands calculated for experimental and theoretical data are presented in Figs. 7–10, respectively. The agreement between theory and experiment is rather good.

In Fig. 11 we show the comparison of the staggering functions for the states of the octupole band ($K^\pi = 1^-$) with the ones of the ground-state band ordered in our way and the previous ($K^\pi = 0^+$) band so far determined as a ground-state band in [4]. In the case of [4] the agreement of the calculated and the experimental data is sensitively worse. The same situation one can find in Fig. 12, where the staggering functions for the octupole ($K^\pi = 2^-$) and ground-state ($K^\pi = 0^+$) bands are compared. To prove that this rearrangement of some states between the S and ground-state bands is not a sort of mere assertion we must analyze the behavior of the $B(E2)$ transitions in the region of the crossing between the ground-state and S bands. Indeed, the transition probabilities even in a simple rigid-rotor model depend on the intrinsic quadrupole moment Q_0, which in our consideration is a function of the number of monopole bosons and increases with increasing n [11]. It will be useful to make a more detailed analysis of the $B(E2)$ transitions, especially in the region of large angular momentum, but unfortunately the lack of experimental data for the lifetimes of the states and transition intensities between them in this region precludes such a possibility.

ACKNOWLEDGMENTS

The investigation was supported by the Bulgarian Science Foundation under Contracts Nos. Φ-1416 and Φ-1501 and in part by the Russian Foundation for Basic Research (RFBR).

[1] C. W. Reich, Nucl. Data Sheets **78**, 547 (1996).

[2] R. B. Firestone, *Table of Isotopes*, 8th ed. (John Wiley & Sons, Inc., New York, 1996), Vol. 2.

[3] J. Adam, Yu. A. Vaganov, V. Vagner, V. P. Volnykh, V. Zvolska, J. Zvolski, Y. S. Ibraheem, T. A. Islamov, V. G. Kalinnikov, B. Kracik, N. A. Lebedev, A. F. Novgorodov, A. A. Solnyshkin, V. I. Stegailov, Zh. Sereeter, M. Fisher, and P. Caloun, BRAS. Phys. **66**, 10 1384 (2002).

[4] A. Jungclaus, B. Binder, A. Dietrich, T. Hartlein, H. Bauer, Ch. Gund, D. Pansegrau, D. Schwalm, J. L. Egido, Y. Sun, D. Bazzacco, G. de Angelis, E. Farnea, A. Gadea, S. Lunardi, D. R. Napoli, C. Rossi-Alvarez, C. Ur, and G. B. Hagemann, Phys. Rev. C **66**, 014312 (2002).

[5] J. Adam, V. P. Garistov, M. Honusek, J. Dobes, J. Zvolski, J. Mrazek, and A. A. Solnyshkin, http://xxx.lanl.gov/archive/nucl-th/0408009.

[6] A. Bohr and B. R. Mottelson, *Nuclear Structure* (Benjamin, New York, 1975), Vol. 4.

[7] R. V. Jolos, Yad. Fiz. **64**, 520 (2001).

[8] R. B. Begzhanov, V. M. Bilenkii, and V. G. Dubro, *Structure of Deformed Nuclei* (in Russian) (Energoatomizdat, Moscow, 1983).

[9] L. K. Peker, S. Pearlstein, J. O. Rasmussen, and J. H. Hamilton, Phys. Rev. Lett. **50**, 1749 (1983).

[10] A. Arima and F. Iachello, Ann. Phys. (NY) **99**, 253 (1976); **111**, 201 (1978).

[11] H. Ganev, V. P. Garistov, and A. I. Georgieva, Phys. Rev. C **69**, 014305 (2004); V. P. Garistov, http://xxx.lanl.gov/archive/nucl-th/0201008; http://xxx.lanl.gov/archive/nucl-th/0008067; http://xxx.lanl.gov/archive/nucl-th/0309058; Nuclear theory, *Proceedings of the XXI Workshop on Nuclear Theory*, edited by V. Nikolaev (Heron Press, Science Series, Sofia, 2002), p. 77; edited by V. Nikolaev (Heron Press, Science Series, Sofia, 2003), p. 305.

[12] A. Georgieva, P. Raychev, and R. Roussev, J. Phys. G: Nucl. Phys. **8**, 1377 (1982); **9**, 521 (1983); A. Georgieva, M. Ivanov, P. Raychev, and R. Roussev, Int. J. Theor. Phys. **28**, 769 (1989).

[13] H. G. Ganev, V. P. Garistov, A. I. Georgieva, and J. P. Draayer, Phys. Rev. C **70**, 054317 (2004).

[14] T. Holstein and H. Primakoff, Phys. Rev. **58**, 1098 (1940); A. O. Barut, *ibid.* **139**, B1433 (1965); R. Marshalek, Phys. Lett. **B97**, 337 (1980); C. C. Gerry, J. Phys. A **16**, 11 (1983).

[15] S. R. Lesher *et al.*, Phys. Rev. C **66**, 051305(R) (2002).